

行政院國家科學委員會專題研究計畫 成果報告

溶膠凝膠法開發新式具高生物活性之彈性複合骨泥(第2年)

研究成果報告(完整版)

計畫類別：個別型
計畫編號：NSC 97-2320-B-040-001-MY2
執行期間：98年08月01日至99年07月31日
執行單位：中山醫學大學口腔生物暨材料科學研究所

計畫主持人：丁信智
共同主持人：陳震漢
計畫參與人員：碩士班研究生-兼任助理人員：賴孟恆
碩士班研究生-兼任助理人員：薛乃碩
博士班研究生-兼任助理人員：何佳哲

報告附件：出席國際會議研究心得報告及發表論文

處理方式：本計畫涉及專利或其他智慧財產權，2年後可公開查詢

中華民國 99 年 08 月 11 日

目錄

1. 中文摘要	2
2. 英文摘要	2
3. Introduction	3
4. Materials and Methods	
4.1. CSC without gelatin	4
4.1.1. Specimen Preparation	4
4.1.2. Characterization of the powders	4
4.1.3. Setting time	4
4.1.4. Compressive strength	4
4.1.5. In vitro soaking	4
4.1.6. Biocompatibility	5
4.2. CSC with gelatin	5
4.2.1. Preparation of the powder containing gelatin	5
4.2.2. Evaluation of anti-washout properties	5
4.2.3. Phase composition and morphology of the cement	6
4.2.4. Diametral tensile strength and modulus measurement	6
4.3. Statistical analysis	6
5. Results	
5.1. Thermal behavior of gel powders	6
5.2. Powder morphology and composition	6
5.3. Cement morphology and composition	7
5.4. Setting time and compressive strength	7
5.5. Characterization of immersed specimens	7
5.6. Biocompatibility of S40C60 cement	7
5.7. Composition and morphology of gelatin-containing cement	8
5.8. Anti-washout properties	8
5.9. Setting time	8
5.10. Diametral tensile strength and modulus	8
6. Discussion	9

1. 中文摘要

發生骨缺損時，病人癒合的必要步驟是經由骨重建以提供骨骼完整機械性。目前臨床上使用玻璃離子體、生物活性玻璃及鈣磷酸鹽骨泥等材料修補骨缺陷，而適合作骨組織修補用的材料必須具備優異生物活性，且與骨組織（主要是由有機相（膠原蛋白）與無機相（氫氧基磷灰石）構成之複合材）相近的結構及機械性。本貳年計劃利用溶膠凝膠法成功發展出水基矽酸鈣骨水泥。研究結果發現鈣矽粉體主要為二鈣矽酸鹽，粉體與水混合之後形成矽酸鈣水和物，硬化時間在 12-42 分鐘之間，並隨前驅物 CaO 含量增加而縮短。在生物活性方面，僅需浸泡模擬體液 1 小時即能析出似骨質的磷灰石球，且其抗壓強度明顯增加。生物相容性顯示 MG63 細胞存活率明顯比對照組增加，且細胞良好貼附於骨水泥材料上面。加入 5% 及 10% 明膠到矽酸鈣骨水泥明顯延長硬化時間 2 及 8 倍；然而，明膠的加入卻大大改善骨水泥的抗沖蝕性與脆性，且沒有不利機械強度。此高活性的矽酸鈣基骨水泥可應用在硬組織修補上。

關鍵詞：骨水泥、矽酸鈣、溶膠凝膠、骨修補、仿生材料

2. 英文摘要

Bone defects occur in a wide variety of clinical situations, and their reconstruction to provide mechanical integrity to the skeleton is a necessary step in the patient's rehabilitation. To date, a variety of materials such as glass-ionomer cement, bioactive glass cement, calcium phosphate-based cement have been clinically evaluated as replacements for damaged hard tissues. In order to be suitable for bone tissue repair, a synthetic material must be biocompatible and it should exhibit some structural and mechanical equivalence to bone that is a composite material consisting mainly of an organic matrix (collagen) and a mineral phase (hydroxyapatite). In the two-year project, novel calcium silicate cements (CSCs) consisting of the sol-gel-derived calcium silicate powder as a solid phase and water as a liquid phase were successfully developed. The results indicated that the dominant phase of β - Ca_2SiO_4 for the SiO_2 -CaO powders increased with an increase in the CaO content of the sols. Setting times for cements mixed with water ranged from 12-42 minutes and were lower for cements with higher starting CaO content. Calcium silicate hydrate (C-S-H) was the principal phase that formed in the hydration process. After immersion in a simulated body fluid as little as 1 hour, the cements were covered with clusters of "bone-like" apatite spherulites. The compressive strength of the immersed cement increased with the increasing time. The MG63 cell viability increased when compared with the control. The cells appeared flat and exhibited intact, well-defined morphology on the cement surface. Addition of gelatin into the CSC significantly prolonged ($P < 0.05$) the setting time by about 2 and 8 times, respectively, for 5% and 10% gelatin. However, the presence of gelatin appreciably improved the anti-washout and brittle properties of the cements without adversely affecting mechanical strength. The development of fast-setting CSCs with high bioactivity may thus have the potential in hard tissue repair.

Keywords: Bone cement, calcium silicate, sol-gel, bone repair, biomimetic materials

3. Introduction

When bone tissue is damaged or fails, a variety of biomaterials are used to achieve a direct chemical bond between bone and bone-repair materials. A self-setting cement composed of only calcium phosphate compounds, which are similar to the mineral component of bone tissue, was developed in the early 1980s and has gained much popularity [1–3]. Calcium phosphate cements (CPCs) that can be injected into bone cavities or defects are good repair materials in orthopedic and dental surgery because of their excellent bioactivity. By increasing their porosity, CPCs may also be used as bone tissue-engineering scaffolds. Thus, limited osteogenic potential may be overcome using calcium phosphate materials.

Silicon, an important trace element in the early stages of bone formation, increased directly with calcium at relatively low calcium concentrations and then fell below the detection limit at compositions approaching hydroxyapatite. The soluble form of silicon may stimulate collagen type I synthesis and osteoblastic differentiation in human osteoblast-like cells. Several attempts have been made to develop silicon-containing biomaterials, such as bioactive glass and silicon-substituted hydroxyapatite (HA), whose silicon component may improve the bioactivity and mechanical properties. The incorporation of silicate ions into HA specifically promoted the processes of bone remodeling at the bone-HA interface.

In general, it could be difficult to deliver to bone defects with complex structures, and hard to compact due to the brittleness of the ceramic cement. Thus, the challenge facing such bioactive ceramic cements is susceptibility to brittle fracture. Additionally, when implanted as a paste that is just starting to set, cements tend to disintegrate upon early contact with blood or other fluids [4]. The washout resistance of the cement plays an important role in successful clinical applications. One strategy to improve the disadvantage could be the use of cohesion promoters such as cellulose, alginate, gelatin, and chitosan to modify the cements [4–10].

Naturally polymeric gelatin is obtained from bovine bone via thermal denaturation or physical and chemical degradation of collagen, and it has been widely employed as a bone graft material [7,8] and as a drug carrier [11] because of its biocompatibility, biodegradability and nontoxicity. Bone and teeth are composite materials composed mainly of an organic matrix (collagen) and a mineral phase (hydroxyapatite). Successful design of bone substitute materials requires an appreciation for the structure of bone. Thus, the synergistic combination of organic and inorganic compounds in hybrid ceramic-polymer biomaterials makes them very useful in hard tissue repair and replacements [5–8]. The use of a hybrid composite made of gelatin and calcium silicate, resembling the morphology and properties of natural bone, may be one way to solve the problem of ceramic brittleness and to enhance the anti-washout properties, all while maintaining good biocompatibility, high bioactivity and bonding properties.

The sol-gels are transformed into ceramics by heating at relatively low temperatures and have better chemical and structural homogeneity than ceramics obtained by conventional glass melting or ceramic powder methods such as solid state sintering. Materials prepared by a sol-gel process are more bioactive than materials of the same compositions prepared by other methods. In this project, the sol-gel technique was used to prepare calcium silicate powders with different molar ratios of SiO_2 :CaO ranging from 7:3–3:7. The calcium silicate cements (CSCs) consisted of calcium silicate powders in solid phase and water in liquid phase. The physiochemical properties of the novel CSCs with and without gelatin before and after a physiological solution was measured. In particular, the proliferation of human osteosarcoma cell line for the cement specimens were also evaluated.

4. Materials and Methods

4.1. CSC without gelatin

4.1.1. Specimen Preparation

Reagent grade tetraethyl orthosilicate ($\text{Si}(\text{OC}_2\text{H}_5)_4$, Sigma-Aldrich, St. Louis, MO) and calcium nitrate ($\text{Ca}(\text{NO}_3)_2 \cdot 4\text{H}_2\text{O}$, Showa, Tokyo, Japan) were used as precursors for SiO_2 and CaO , respectively. Nitric acid was used as the catalyst and ethanol as the solvent. For simplicity, throughout this study, the sintered powders and the cements derived from such powders were designated by the same codes, as listed in Table 1. Briefly, $\text{Si}(\text{OC}_2\text{H}_5)_4$ was hydrolyzed with the sequential addition of 2 mol/L HNO_3 and absolute ethanol with 1 hour of stirring separately. The required amount of $\text{Ca}(\text{NO}_3)_2 \cdot 4\text{H}_2\text{O}$ was added to the above solution and the mixed solutions were stirred for an additional hour. The sol solution was sealed and aged at 60°C for 1 day. After which, vaporization of the solvent in an oven at 120°C was for at least 2 days to obtain an as-dried gel. Based on the TGA–DSC results, the as-dried gel was heated in air to 800°C at a heating rate of $10^\circ\text{C}/\text{min}$ for 2 h using a high-temperature furnace and then cooled to room temperature in the furnace to produce a powder. The sintered granules were then ball-milled for 12 hours in ethyl alcohol using a Retsch S 100 centrifugal ball mill (Hann, Germany) and dried in an oven at 60°C .

4.1.2. Characterization of the powders

After vaporization of the solvent in an oven at 120°C following aging, a Netzsch DSC 404 (Gerätebau, Germany) was used to acquire the thermal events occurring. Thermal stability was determined by TGA using a Seiko SSC 5000 system (Chiba, Japan). Both thermal analyses were started from room temperature at a heating rate of $10^\circ\text{C}/\text{min}$ in air up to 1000°C . SEM (JEOL JSM-6700F, Tokyo, Japan) was used to characterize morphology of the powders. To investigate the phase composition, the specimens were ground to fine powders and then characterized with an X-ray diffractometer (XRD, Shimadzu XD-D1, Kyoto, Japan). Fourier transform infrared spectroscopy (FTIR, Bomem DA8.3, Hartman & Braun, Canada) was used to analyze the powders.

4.1.3. Setting time

All specimens were hand-mixed at a liquid-to-powder (L/P) ratio of 0.5 g/mL with distilled water as the liquid phase. After mixing, the cement was placed into a cylindrical stainless steel mold (diameter = 6 mm and height = 12 mm) and stored in an incubator at 100% relative humidity and 37°C . The setting times of the cements were tested using a 400-G Gillmore needle with a 1-mm diameter, according to ISO 9917-1 for water-based cements.

4.1.4. Compressive strength

Compressive strength (CS) was measured on an EZ-Test machine (Shimadzu, Kyoto, Japan) at a loading rate of 0.5 mm/minute.

4.1.5. In vitro soaking

The specimens were hand-mixed at a liquid-to-powder (L/P) ratio of 0.5 g/mL with distilled water as the liquid phase and placed into a cylindrical Teflon mold (diameter = 6 mm and height = 12 mm). Each specimen was stored in an incubator at 100% relative humidity and 37°C for 1 day and then was immersed in 10 mL simulated body fluid at 37°C . The solution suggested by Kokubo, which ionic composition is similar to that of human blood plasma, consisted of 7.9949 g NaCl, 0.3528 g NaHCO_3 , 0.2235 g KCl, 0.147 g K_2HPO_4 ,

0.305 g $\text{MgCl}_2 \cdot 6\text{H}_2\text{O}$, 0.2775 g CaCl_2 , 0.071 g Na_2SO_4 in 1000 ml distilled H_2O and was buffered to pH 7.4 with hydrochloric acid (HCl) and trishydroxymethyl aminomethane ($(\text{CH}_2\text{OH})_3\text{CNH}_2$). All chemicals used were of reagent grade and used as obtained. The solution in a shaker water bath was not changed daily. After immersion periods of 1, 7, and 30 days, specimens were removed from the vials to evaluate the *in vitro* properties.

4.1.6. Biocompatibility

Cement biocompatibility was evaluated by incubating the cement specimens with MG63 human osteoblast-like cells (BCRC 60279, Hsinchu, Taiwan). Prior to cell incubation, the hardened cement discs were sterilized by soaking in a 75% ethanol solution and exposure to ultraviolet (UV) light for 2 hours. MG63 cells were suspended in Dulbecco's Modified Eagle's Medium (DMEM, Gibco, Langley, OK) containing 10% Fetal bovine serum (Gibco), 1% penicillin (10,000 U/ml)/streptomycin (10,000 mg/ml) solution (Gibco), 0.01 M glycerol-2-phosphate (Sigma, St. Louis, MO), 2.84×10^{-4} M L-ascorbic acid (J.T. Baker, Phillipsburg, NJ), and 10^{-10} M dexamethasone (Sigma). MG63 suspensions (2×10^4 cells per well) were directly seeded over each cement specimen, which was then placed in a 24-well plate. Cell cultures were incubated at 37°C in a 5% CO_2 atmosphere. The Cell Proliferation Reagent WST-1 (Roche Diagnostics, Mannheim, Germany) was used to assess cell viability, which was based on the cleavage of a tetrazolium salt (WST-1) by the mitochondrial dehydrogenase of living cells. Briefly, 3 hours before the end of incubation, 100 μL of WST-1 solution (Sigma) and 900 μL of medium were added to each well. 200 μL of the solution in each well was transferred to a 96-well tissue culture plate. Plates were read in a Sunrise Microtiter Reader (Tecan Austria Gesellschaft, Salzburg, Austria) at 440 nm with a reference wavelength of 650 nm. Sample analysis results were obtained in triplicate from three separate experiments. MG63 cultured on tissue culture plates (TCPs) were used as a control. The cell viability was normalized to the TCPs in terms of optical density (OD). After incubation for 3 days, the cement specimens were washed with phosphate-buffered saline (PBS) three times and fixed in 2% glutaraldehyde for 3 hours. The specimens were then dehydrated using a graded ethanol series for 20 min at each concentration and dried with liquid CO_2 using a critical point dryer device (LADD 28000, LADD, Williston, VT). The dehydrated specimens were mounted on stubs, coated with gold, and inspected using a SEM/

4.2. CSC with gelatin

4.2.1. Preparation of the powder containing gelatin

To prepare the organic-inorganic composite, type B gelatin (isoelectric point at pH = 4.7–5.2) from bovine skin (Sigma-Aldrich) was added to the sintered powder at either 5% or 10% by weight using a conditioning mixer (ARE-250, Thinky, Tokyo, Japan). The mixtures were then ball-milled for 12 h in ethanol using a Retsch S 100 centrifugal ball mill and dried in an oven at 60°C before use.

4.2.2. Evaluation of anti-washout properties

To prepare the cement, the liquid-to-powder (L/P) ratios of 0.45, 0.5, 0.55 and 0.6 (mL/g) were adopted for the S60C40, S50C50, S40C60, and S30C70 systems, respectively. The variations in L/P depended on the Ca content because a greater amount of liquid was needed to harden the powder with the higher Ca content. The cement without gelatin was as the control. Anti-washout properties of the cement specimens were evaluated by visual observation. After mixing, the cements were molded in a stainless steel mold to form the

cylindrical specimen dimension of 6 mm (diameter) × 3 mm (height). This size was adopted throughout the study, unless described elsewhere. They were then taken out and immediately placed into a SBF at 37°C. The test specimens were considered to have passed the washout resistance test if the cement did not visibly disintegrate in the solution after 1 h.

4.2.3. Phase composition and morphology of the cement

To analyze phase composition, morphology and mechanical properties of the cements, they were incubated in a 37°C and 100% humidity environment and allowed to set for 1 day. Phase analysis of the cement specimens was performed using an XRD operated at 30 kV and 30 mA at a scanning speed of 1°/min. The surfaces of the cement specimens were coated with gold using a JFC-1600 coater and examined under a JSM-6700F SEM operated in the lower secondary electron image (LEI) mode at 3 kV accelerating voltage.

4.2.4. Diametral tensile strength and modulus measurement

DTS testing was performed on an EZ-Test machine at a loading rate of 0.5 mm/min after the powder was mixed with water and set for 1 day in a 37°C and 100% humidity environment, as described above. The DTS value of each cement specimen was calculated using the relationship defined in the equation $DTS = 2P/\pi bw$, where P is the peak load (Newtons), b is the diameter (mm) and w is the thickness (mm) of the specimen. The maximum load at failure was obtained from the recorded load-deflection curve. The elastic modulus of the cement specimens was determined from the slope of the linear elastic portion of the load-deflection curve. At least twenty specimens from each group were tested. The interior surface (fractured surface) after diametral tensile loading was also examined by SEM.

4.3. Statistical analysis

One-way analysis of variance (ANOVA) was used to evaluate significant differences between means in the measured data. Scheffe's multiple comparison testing was used to determine the significance of standard deviations in the measured data from each specimen under different experimental conditions. In all cases, results were considered statistically significant with a *p*-value of less than 0.05.

5. Results

5.1. Thermal behavior of gel powders

Figure 1 shows the TGA–DSC curves of the as-dried gel powders. The four specimens showed similar thermal behavior, indicating that the first weight loss of about 10% was found, followed by continuous weight loss from 100 to 450°C in the TGA curve. The decomposition and oxidation of the decomposed products were accelerated at temperatures of 450–550°C, as evidenced by a rapid weight loss of more than 30%. In the DSC traces, there were four endothermic peaks at about 100, 520, 540, and 650°C, and one exothermic peak at about 900°C.

5.2. Powder morphology and composition

The particle size of powders is an important characteristic, and therefore it was analyzed by SEM. In Figure 2, the SEM micrograph shows all of the milled particles before mixing with water to essentially be an assembly of irregular particles with sizes ranging from 0.5 to 5 μm. The more CaO contents the powders contained, the smaller the particle size was. Additionally, the powers with higher SiO₂ contents presented a denser structure.

Figure 3A shows the XRD patterns of the 5 SiO₂–CaO powders sintered at 800°C and indicates that the phase evolution is dependent on the Si/Ca ratio of the precursors. The major diffraction peaks at 2θ between 32° and 34° were attributed to the β-dicalcium silicate (β-Ca₂SiO₄) phase. The peak intensities of β-Ca₂SiO₄ and CaO increased with increasing CaO content in the precursors. The trends in the FTIR spectra (Fig. 3B) are similar to those indicated by XRD. For the specimen with the greatest amount of silica (S70C30), the broad IR absorption band corresponding to SiO₄ asymmetric stretching extended over a wide wavenumber range of 1300–950 cm⁻¹. An obvious sharpening and shifting to lower frequency in Si–O–Si asymmetric stretching bands were detected as the silica content decreased.

5.3. Cement morphology and composition

When the powder solid was mixed with water, the products of the hydration process were C–S–H at 29.3° and incompletely reacted inorganic component phases (Fig. 4A). The lower Si/Ca ratio was in the precursor, the higher the C–S–H content was in the cement. Except S70S30 cement, which had a loose and rough surface (Fig. 4B), all other specimens had a smooth appearance with entangled particles (Fig. 4C–4F). Moreover, it seemed that S50C50 had a denser structure than the other cements.

5.4. Setting time and compressive strength

The setting times of the five CSC cements ranged from 12–42 minutes (Table 1); these values were significantly different ($P < .05$). Table 1 also shows the CS values of cement specimens. One-way ANOVA analysis of the CS data shows that the variations in strength between specimens are significant ($P < .05$).

5.5. Characterization of immersed specimens

Broad face SEM micrographs and EDS profile of S40C60 cement specimens immersed in a simulated body fluid for 1 hour are shown in Figure 5. It is clear that, precipitation took place on the cement surface which was covered with clusters of precipitated spherulites (Fig. 5A). The Ca/P and Ca/Si ratios of the cement specimen after 1 hour of immersion were 1.98 and 6.19 (Fig. 5B), respectively.

When the powder solid is mixed with water, the products of the hydration process are C–S–H at 29.3° and incompletely reacted inorganic component phases (Fig. 6A). Additionally, the diffraction peaks at 2θ between 32.0° and 34.5° were attributed to the β-Ca₂SiO₄ phase. After immersion in simulated body fluid, it can be easily seen that the intensities of the β-Ca₂SiO₄ phase gradually reduced. Some broad and diffuse peaks at 2θ = 25.9° as well as 31.8–32.9° appeared instead, which may be ascribed to the characteristic peaks of apatite. Interestingly, the patterns also showed that the relative peak intensity of the C–S–H component of the day 1 specimen was higher than that of the day 0 specimen.

The changes in compressive strength of S40C60 cement specimens after immersion in simulated body fluid as a function of time are shown in Figure 6B. The values at 0-, 1-, 7-, and 30-day immersion in a simulated body fluid were 12.3 ± 2.3, 20.2 ± 2.8, 23.0 ± 3.4, and 22.3 ± 1.6 MPa, respectively. The immersed specimens were significantly ($p < 0.05$) higher than that obtained for the day 0 specimens.

5.6. Biocompatibility of S40C60 cement

In Figure 7A WST-1 assay shows that the cell viability increased 15% and 23% at 6-hour and 7-day incubation, respectively, when compared with the controls. The SEM image reveals

cells that appeared flat and exhibited intact, well-defined morphology (Fig. 7B).

5.7. Composition and morphology of gelatin-containing cement

XRD patterns of all cements revealed an obvious diffraction peak around $2\theta = 29.4^\circ$, corresponding to the calcium silicate hydrate (C–S–H) gel, and incompletely reacted inorganic component phases of β - Ca_2SiO_4 (Fig. 8). It is clear that the peak intensity of C–S–H formed in the gelatin-containing cement specimen was lower, in particular for 10% gelatin, when compared with the corresponding control. The SEM micrographs of the cements with and without 10% gelatin indicated that the as-set CSC controls had an appearance with entangled particles and exhibited several pores. A dense structure appeared for the cement with larger CaO amounts in the sol. In contrast, when 10% gelatin was added, the organic-inorganic hybrid cements became more compact than the corresponding cements without gelatin.

5.8. Anti-washout properties

Washout resistance results indicated that the four controls appeared to degrade after immersion. It can clearly be seen that the gelatin hybrid cements resisted washout, showing no noticeable breakdown.

5.9. Setting time

After mixing with water, the control cements set in the range of 10 to 29 min, which were shortened with an increase in the concentration of the calcium component, as shown in Figure 6. These values were significantly ($P < 0.05$) different from each other. Scheffe's multiple comparison testing revealed no significant difference ($P > 0.05$) between S30C70 and S40C60. It was also not significant different ($P > 0.05$) for the S50C50 and S60C40 control. The addition of 5% and 10% gelatin significantly ($P < 0.05$) prolonged the setting time of the hybrid cements by a factor of about 2 (25–69 min) and 8 (108–282 min), respectively. In the case of CSCs containing either 5% or 10% gelatin content, setting time had significant differences ($P < 0.05$) between various CSCs.

5.10. Diametral tensile strength and modulus

Figure 9 shows that the DTS values of the hardened control cements were 2.0, 2.6, 2.0, and 1.0 MPa with an increasing CaO content, indicating there was a significant difference ($P < 0.05$). The incorporation of gelatin into the CSC did not significantly affect ($P > 0.05$) its strength, which was comparable to that of the control cement. In the case of S40C60 group, the DTS values were 2.0, 2.1, and 1.7 MPa for 0, 5, 10% gelatin content, respectively. The significant differences ($P < 0.05$) in DTS between S40C60 and S60C40 groups were not found. On the other hand, Scheffe's multiple comparison testing indicated that both 5% and 10% gelatin-containing S50C50 cement specimens had significantly ($P < 0.05$) higher DTS values than the other CSC systems with and without gelatin, with the exception of the S50C50 control.

The values of the mean elastic moduli obtained during the measurement of diametral tensile strength are also shown in Figure 11 along with the respective standard deviations. The elastic moduli of the CSC systems with and without gelatin in the range of 26.8–43.3 MPa presented significant differences ($P < 0.05$). It was found that the S50C50 control had an insignificantly higher modulus than the other three CSC controls ($P > 0.05$). The modulus decreased somewhat after the incorporation of either 5% or 10% gelatin to the CSC control, but there was not significantly different ($P > 0.05$) for the same CSC system after Scheffe's

multiple comparison testing.

6. Discussion

The sol-gel technique was used to prepare 5 different calcium silicate powders. TGA and DSC were used to define the sintering temperatures of the as-prepared $\text{SiO}_2\text{-CaO}$ gel specimens. All powder specimens indicated a first weight loss of about 10%, where a broad endotherm was observed at around 100°C . This was due to evaporation of residual or absorbed solvent, pore liquid and crystalline water in the $\text{Ca}(\text{NO}_3)_2\cdot 4\text{H}_2\text{O}$ precursor. The continuous weight loss from 100 to 450°C was suggested to be due to the decomposition of organic species produced from hydrolysis/condensation reactions, which are accelerated at $400\text{--}550^\circ\text{C}$, as evidenced by rapid weight loss of more than 30% in this temperature range. There was no appreciable weight loss observed above 700°C , indicating that the precursors may generate a phase after heat-treatment at temperatures more than 700°C . In the DSC curves, the endothermic peaks in the range of $520\text{--}540^\circ\text{C}$ were caused by the condensation of silanol groups and the release of nitrate groups introduced as calcium nitrate in the preparation of the sol, which was consistent with the results of the TGA. The endothermic peak around 650°C was ascribed to the chemical reactions between the precursors, which may lead to the formation of a crystalline phase. Based on the TGA–DSC data, thermal treatment at 800°C for 2 h in air was used to prepare the $\text{SiO}_2\text{-CaO}$ powders.

The XRD analyses indicated that S70C30, containing the highest amount of SiO_2 , had an amorphous phase without characteristic peaks. With a greater amount of CaO than SiO_2 , the diffraction peaks of $\beta\text{-Ca}_2\text{SiO}_4$ became stronger, even with a small total amount of CaO. Similarly, the CaO peak intensities increased with increasing CaO content of the powders. In the FTIR spectra, the broad band of $1300\text{--}950\text{ cm}^{-1}$ further split into two appreciable adsorption bands, indicating increased crystallinity with increasing CaO content, which is in agreement with the XRD results. A new band at 850 cm^{-1} emerged that was associated with the Si–O symmetric stretching mode with one non-bridging silicon–oxygen bond (Si–O–NBO). The band at $550\text{--}500\text{ cm}^{-1}$ originated from the vibration of the siloxane backbone. The presence of Ca^{2+} as the network modifier in the silicates led to a disruption in the continuity of the glassy network due to breaking of some of the Si–O–Si bonds and resulted in the formation of Si–O–NBO. The bands between 1550 and 1380 cm^{-1} may have arisen from the vibrational mode of the CO_3 group, which came from atmospheric carbonation. The XRD and FTIR results of the powders consistently indicated calcium amounts significantly affected the phase evolution.

The present CSCs exhibited distinctly shortened setting times. Particle size, sintering temperature, liquid phase, and composition of powders, as well as the ratio of liquid to powder, played crucial roles in the setting time of the paste materials. When the powder and liquid phase were mixed in an appropriate ratio, they formed a paste that hardened by entanglement of the crystals precipitated in the paste at body or room temperature. The entanglement structure, consisting of fine particle agglomerates, could be considered a hydration product of a C–S–H gel that may be responsible for causing the particles to adhere to one another. The cement specimen with the greatest SiO_2 content (S70C30) had a compressive strength of only 0.3 MPa, while the specimen with the lowest SiO_2 content (S30C70) reached the strength of 3.2 MPa. It is worth noting that the highest CS value was 15.2 MPa and belonged to the equimolar ratio of SiO_2/CaO (S50C50), which appeared denser in structure than the others.

After immersion in a simulated body fluid for as little as 1 h, the cement specimens

induced the precipitation of apatite spherulites, indicating its high bioactivity. To further confirm that the observed apatite layer was indeed precipitated from simulated body fluid, a SEM/EDS analysis was performed on the immersed surface. This precipitate has been identified to be apatite although a Ca/P ratio of 1.98. The much higher Ca/P ratio (than the stoichiometric Ca/P ratio, 1.67, of apatite) on 1-hour-immersed surfaces was not surprising due to the fact that a large quantity of calcium originated from the underlying cement was detected. This result may be interpreted by the presence of Si because the Ca/Si ratio (stoichiometric ratio of 1.5 used in the sol) of the immersed specimen was 6.19. The bioactive behavior of the SiO₂-CaO-based cement indicated that the presence of phosphorous in the composition was not an essential requirement for the development of a carbonated apatite layer. This was because the phosphorous originated from the *in vitro* assay solution.

The S40C60 cement specimen had an original strength of 12.3 MPa. Upon immersion in a simulated body fluid, the cements reached their higher value of the compressive strength, was similar to the changes in phase transformation in term of XRD patterns. Contrary to day 0 specimens, one-way ANOVA analysis of the compressive strength data showed that the day 1 specimens significantly increased the strength by an approximately two-fold factor. Another finding that deserved attention was the fact that simulated body fluid did not adversely affect the compressive strength values of the cement, even after 30 days of immersion, indicating that there was no *in vitro* degradation of bond strength. The immersion-induced increase in mechanical strength was possibly attributable to the more complete hardening during immersion in solution, which has also been observed in other studies.

To elucidate the effect of the cement on the osteogenesis induced by osteoblast cells, the morphology, attachment, and proliferation of MG63 cells were evaluated. The cell were spreading and flattening on the cement surface, representing the survival of MG63 cells on the cement. Early cell-cement interactions affected subsequent differentiation and mineralization. Cells attached to the cements at a rapid rate more than 100 % binding within the 6 hours compared to the control, demonstrating that the number of viable cells on cement surfaces was significantly higher than on TCPs. The increased attachment and proliferation of MG63 cells showed that S40C60 cement could provide an optimal environment for osteoblasts to function normally, consistent with the earlier immersion results.

The added gelatin may play a crucial role in the properties of the hybrid cements. A colloidal gel formed a dense structure of hydrated hybrid cement that entangled the original C-S-H structure. Such a dense structure of gelatin-containing cements might be due to the existence of negatively charged gelatin. Type B gelatin with an isoelectric point of about 5 has a high density of carboxyl groups, which makes the gelatin negatively charged. The carboxyl groups might bind calcium ions on the surface of calcium silicate particles. Hence, more entanglements were formed between the inorganic particles and concrete cement bodies. The enhanced structure may improve the washout and brittle properties of the CSC. On the other hand, the reaction could inhibit C-S-H formation. This might explain why the presence of gelatin in the cement specimen apparently reduced the peak intensity of C-S-H at $2\theta = 29.4^\circ$ and prolonged the setting time.

The paste of the four control cements without gelatin could be washed out completely when immersed in SBF immediately after mixing. In contrast, the gelatin hybrid cements resisted washout. Although the detailed mechanisms of washout resistance for gelatin-containing CSCs have not been fully clarified at present, the improvement in anti-washout properties can be attributed to the adhesive property and negative charge of gelatin, which serves as a 'glue' to fuse the particles together. The physical reaction may prohibit the penetration of cement paste by liquid, which is considered a cause of the washing out

properties of cement pastes, thus endowing the gelatin-containing CSCs with anti-washout ability. The polymeric gelatin materials have the potential to improve the anti-washout properties of CSCs.

The addition of 5% and 10% gelatin prolonged the setting time of the hybrid cement by up to about 2 and 8 times, respectively, indicating the adverse effect of gelatin on the hardening reaction of CSCs. For example, S50C50 had setting times of 55 and 136 min when containing 5% and 10% gelatin, respectively, from the original 23 min of the control without gelatin. Naturally polymeric gelatin absorbs the water and forms a gel that partially encapsulates the particles and impedes the hydration reaction of the CSC. The resulting hardening properties of the hybrid cements would be a combination between the progressive hardening due to the main calcium silicate reactant and the progressive complex reaction, such as intramolecular hydrogen bonding between water and the gelatin phase. Wang *et al.* reported that excessive polyanions destroy the balance of cement components within a ceramic cement, leading to very slow setting processes or no setting at all [12]. Polymer interactions with cement and their contributions to the hydration reaction are far from being clarified and deserve further investigation, despite the evident importance of additives.

The four CSC systems could give C–S–H as the final product after their powder phases were mixed with water. However, their DTS results were significantly different; for example, 2.6 MPa for S50C50 and 1.0 MPa for the fastest setting S30C70. Although the detailed mechanism underlying the changes in DTS has not been fully clarified, it seemed that at least two factors, i.e. a formed C–S–H and remaining reacted phase structure, were operating competitively to determine the eventual strength level of the four cements. XRD patterns also indicated that there were incompletely reacted inorganic component phases of β -Ca₂SiO₄ in the set cement specimen, in addition to hydration product of C–S–H. Nevertheless, the denser and quickest-setting S30C70 cement had the lowest strength among the four control groups possibly due to weak cohesion within unreacted microstructure, as indicated in particle morphology with a fragile type (Fig. 1), which might lead to an intragranular fracture. The increasing gelatin content did increase the ductility of CSC, while the mean fracture strength and modulus showed only small changes with no significant differences. On the other hand, the values of the mean elastic moduli were 43.3, 34.5, and 36.6 MPa for the control, 5%, and 10% gelatin-containing cements, respectively, indicating no differences were found.

References

1. Brown WE, Chow LC. Dental restorative cement pastes. US Pat. No. 4,518,430, 1985.
2. Miyamoto Y, Ishikawa K, Fukao H, Sawada M, Nagayama M, Kon M, Asaoka K. In vivo setting behaviour of fast-setting calcium phosphate cement. *Biomaterials* 1995;16:855–60.
3. Welch RD, Zhang H, Bronson DG. Experimental tibial plateau fractures augmented with calcium phosphate cement or autologous bone graft. *J Bone Joint Surg Am* 2003;85:222–31.
4. Wang X, Chen L, Xiang H, Ye J. Influence of anti-washout agents on the rheological properties and injectability of a calcium phosphate cement. *J Biomed Mater Res B*. 2007;81:410–8.
5. Ishikawa K, Miyamoto Y, Takechi M, Toh T, Kon M, Nagayama M, Asaoka K. Non-decay type fast-setting calcium phosphate cement: Hydroxyapatite putty containing an increased amount of sodium alginate. *J Biomed Mater Res*. 1997;36:393–9.
6. Ito M, Yamagishi T, Yagasaki H, Kafrawy AH. In vitro properties of a chitosan-bonded bone-filling paste: studies on solubility of calcium phosphate compounds. *J Biomed Mater*

- Res. 1996;32:95–8.
7. Fujishiro Y, Takahashi K, Sato T. Preparation and compressive strength of α -tricalcium phosphate/gelatin gel composite cement. *J Biomed Mater Res.* 2001;54:525–30.
 8. Panzavolta S, Fini M, Nicoletti A, Bracci B, Rubini K, Giardino R, Bigi A. Porous composite scaffolds based on gelatin and partially hydrolyzed α -tricalcium phosphate. *Acta Biomater.* 2009;5:636–43.
 9. Khairoun I, Driessens FCM, Boltong MG, Planell JA, Wenz R. Addition of cohesion promoters to calcium phosphate cements. *Biomaterials.* 1999;20:393–8.
 10. Cherng A, Takagi S, Chow LC. Effects of hydroxypropyl methylcellulose and other gelling agents on the handling properties of calcium phosphate cement. *J Biomed Mater Res.* 1997;35:273–7.
 11. Olsen D, Yang C, Bodo M, Chang R, Leigh S, Baez J, Carmichael D, Perälä M, Hämäläinen ER, Jarvinen M, Polarek J. Recombinant collagen and gelatin for drug delivery. *Adv Drug Delivery Rev.* 2003;55:1547–67.
 12. Wang XH, Feng QL, Cui FZ, Ma JB. The effects of S-chitosan on the physical properties of calcium phosphate cements. *J Bioact Compat Polym.* 2003;18:45–57.

Table 1. Composition (molar ratio), setting time (Ts) and compressive strength (CS) of the five calcium silicate cements after mixing with water

Specimen Code	Composition (SiO ₂ :CaO)	Ts (min)	CS (MPa)
S70C30	7:3	42 ± 2 ^a	0.3 ± 0.1 ^f
S60C40	6:4	31 ± 2 ^b	9.4 ± 2.1 ^g
S50C50	5:5	24 ± 2 ^c	15.2 ± 2.5 ^h
S40C60	4:6	16 ± 2 ^d	12.0 ± 2.6 ⁱ
S30C70	3:7	12 ± 2 ^e	3.2 ± 0.5 ^j

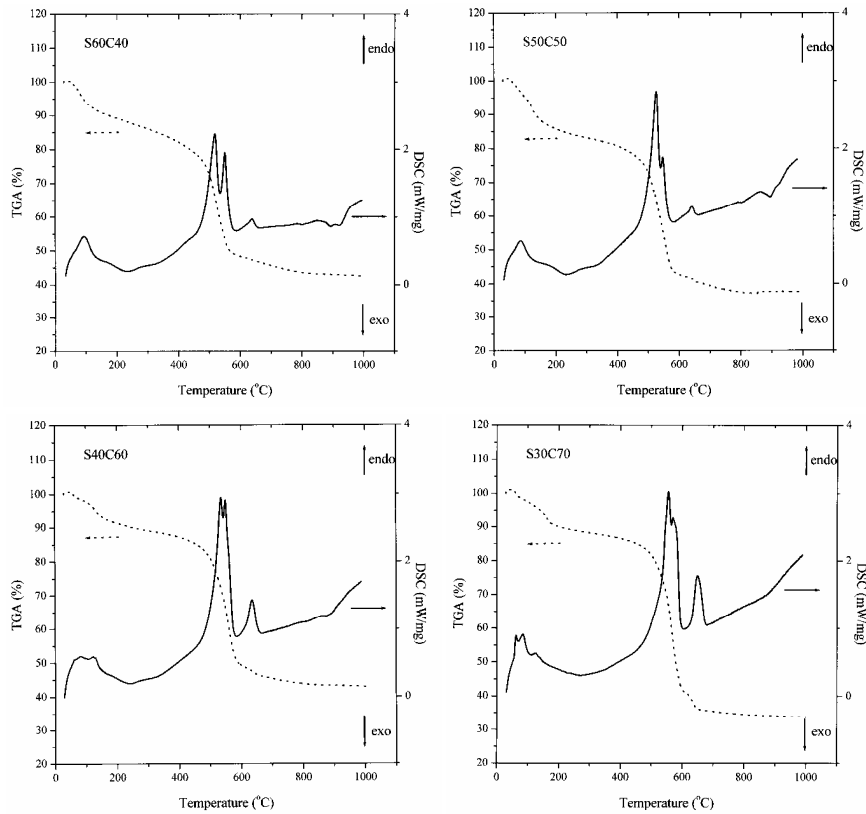


Figure 1 TGA–DSC traces for S60C40, S50C50, S40C60 and S30C70 gel powders that have been dried at 120°C.

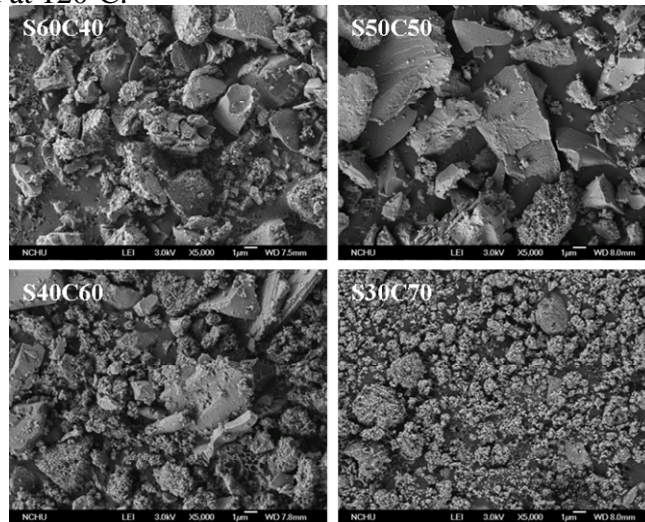


Figure 2 SEM micrographs of various ground powders sintered at 800°C.

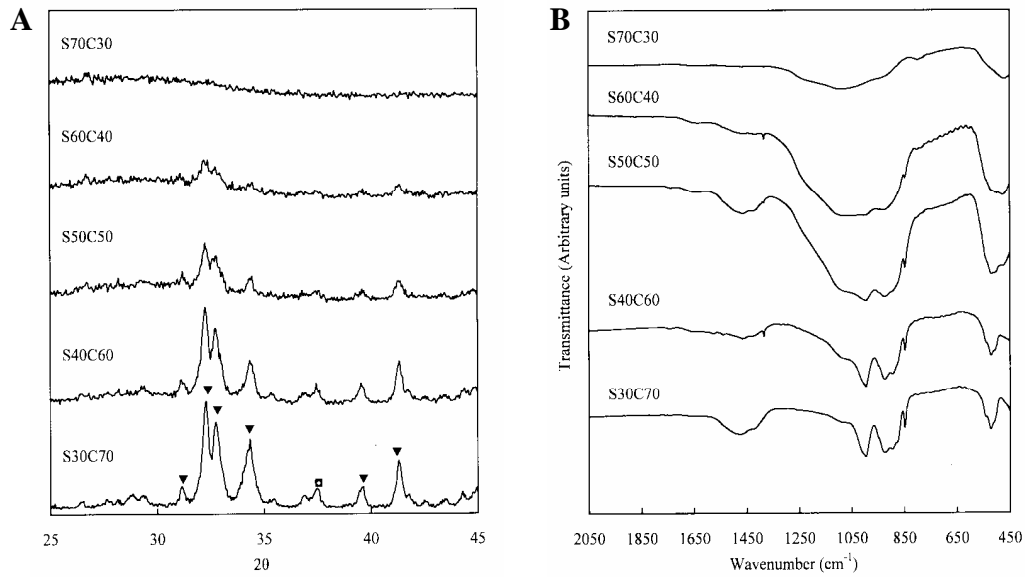


Figure 3 (A) X-ray diffraction patterns and (B) Fourier transform infrared spectra of 5 calcium silicate powders sintered at 800°C. \blacksquare : CaO; \blacktriangledown : β -Ca₂SiO₄.

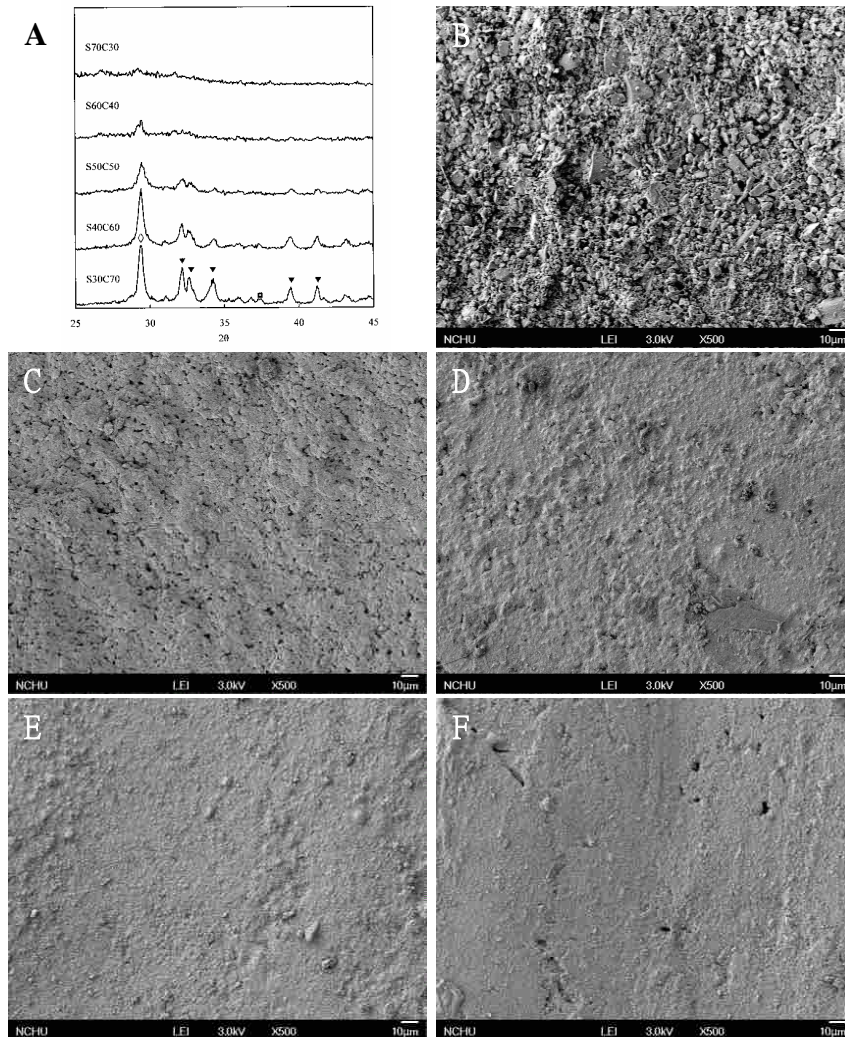


Figure 4 (A) X-ray diffraction patterns of 5 CSCs. Scanning electron micrographs of (B) set S70C30, (C) S60C40, (D) S50C50, (E) S40C60, and (F) S30C70 cements. \blacksquare : CaO; \blacktriangledown : β -Ca₂SiO₄; \blacklozenge : C-S-H.

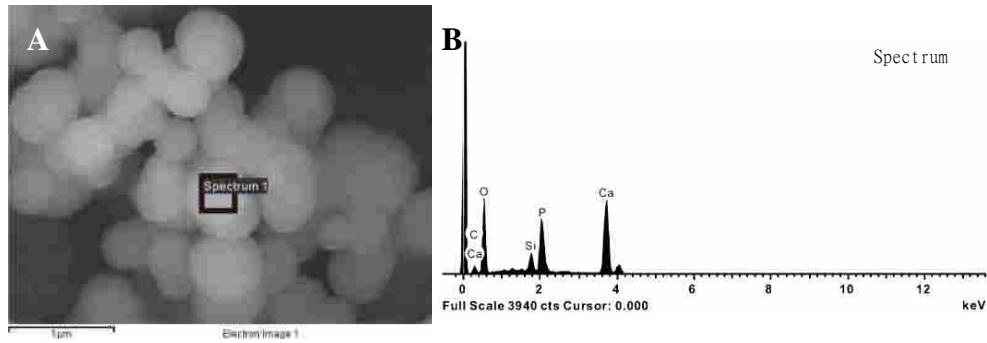


Figure 5 (A) Morphology and (B) elemental analysis selected from the square area of the morphology after soaking in a simulated body fluid for 1 hour.

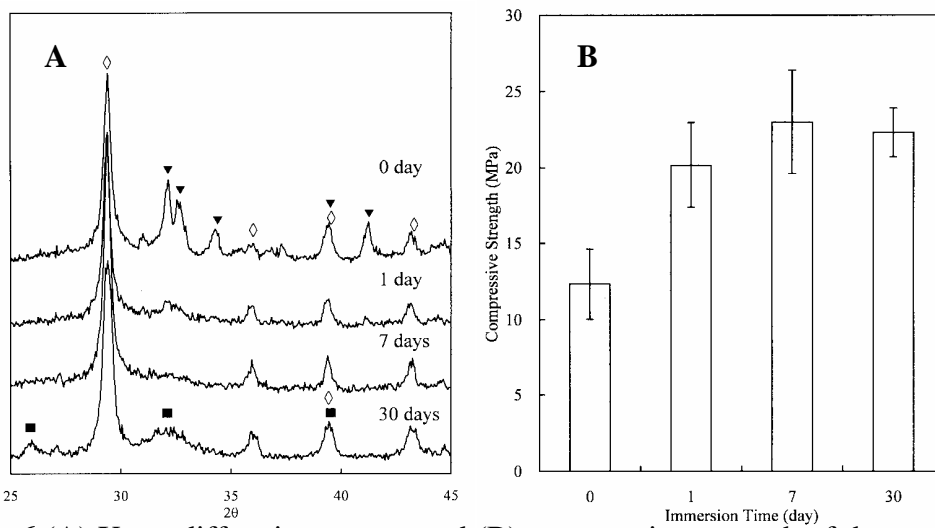


Figure 6 (A) X-ray diffraction pattern and (B) compressive strength of the cement specimens before and after immersion in a simulated body fluid (0, 1, 7, 30 days). \blacktriangledown : β - Ca_2SiO_4 ; \diamond : C-S-H; \blacksquare : apatite.

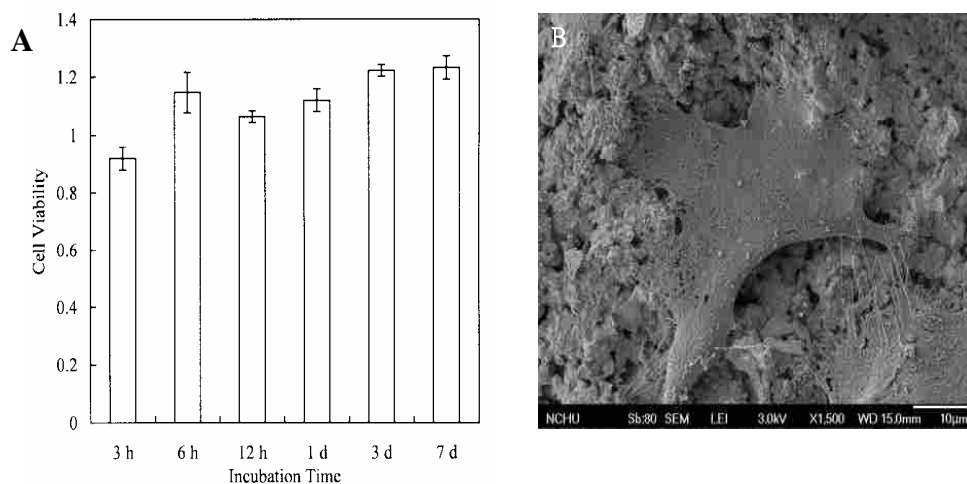


Figure 7 (A) WST-1 assay MG63 cell viability cultured on the cement specimens at various time periods. (B) Cell morphology of MG63 cultured on the cement surfaces at 3 days.

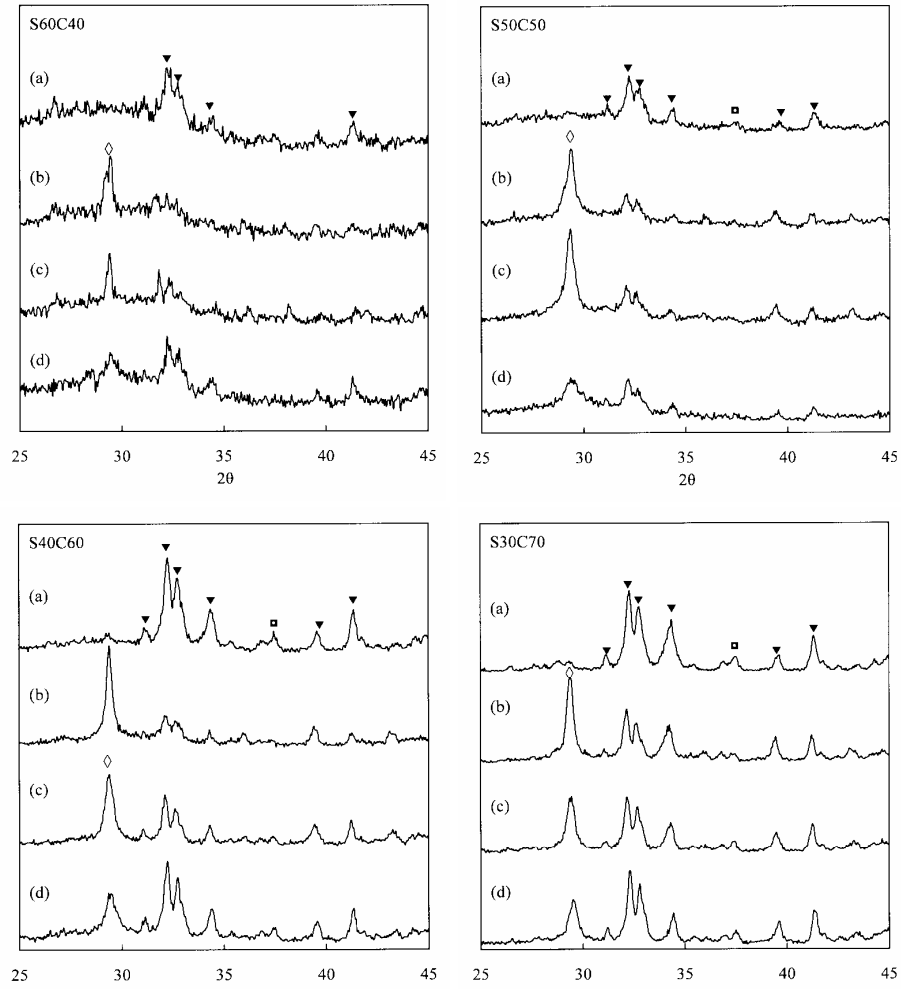


Figure 8 XRD patterns of the four CSC systems. (a) Powder, (b) cement without gelatin, (c) cement containing 5 wt% gelatin, and (d) cement containing 10 wt% gelatin. \blacksquare : CaO; \blacktriangledown : β - Ca_2SiO_4 ; \diamond : C-S-H.

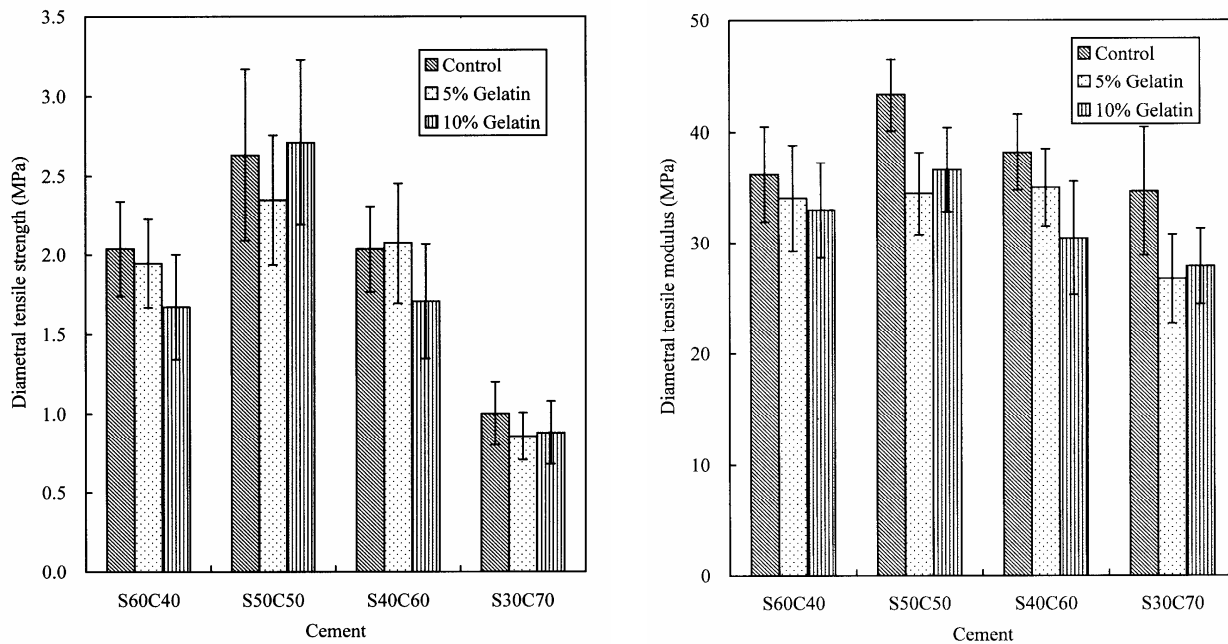


Figure 9 DTS and modulus of various CSCs with and without gelatin.

出席國際學術會議心得報告

計畫編號	NSC 97-2320-B-040-001-MY2
計畫名稱	溶膠凝膠法開發新式高生物活性之彈性複合骨泥
出國人員姓名 服務機關及職稱	丁信智 中山醫學大學 口腔生物暨材料科學所 教授
會議時間地點	97/9/7-97/9/11 瑞士 洛桑
會議名稱	2009 年第 22 屆歐洲生醫材料大會
發表論文題目	Properties of Injectable Calcium Silicate Hybrid Cements

一、參加會議經過

本年第 22 屆歐洲生醫材料研討會在瑞士洛桑的國際會議廳舉行。發表分口頭 (256 篇) 及海報貼示 (752 篇)，超過 1000 篇，並有 4 場 workshop (共 20 位專家報告)，會議期間每天有 J. Leray 及 G. Winter 獎得獎者的專題演講。整個會議研討涵蓋與生醫材料相關的各種不同議題，如組織工程、表面修飾、仿生材料、鈣磷陶瓷、降解性高分子、生物相容性研究、蛋白質吸附、奈米複合材、基因藥物治療研究等。並有生醫材料製造、儀器設備商、及書商同時參展，會場討論氣氛十分熱絡。

二、與會心得

此研討會主要是由歐洲生醫材料學會主導，除歐洲地區生醫材料學者參加外，美加及亞洲地區多位學者亦參與。台灣學者除我本人外，另有來自中興材料系所的師生參加。生醫材料研究為一跨領域且理論、應用並重的學門，從與會中所發表的論文可知仍有相當大的研究空間，但有待臨床醫師與生醫材料研究者雙向交流與合作，才能更加突破目前所面臨之瓶頸。從國外學者的研究趨勢及發表主題，顯示台灣生醫材料界研究方向與世界並進、並未偏離。本次參與研討會也與國外學者進行多次意見交流。這次本人的論文發表有幸被遴選在紀念 Prof. Ferdinand Driessens 會場上，口頭發表矽酸鈣骨水泥。Prof. Ferdinand Driessens 是西班牙知名的磷酸鈣骨水泥專家，在 1982 年首先提出磷酸鈣骨水泥 (早於 1983 年 Chow)，其後發表了近 300 篇骨水泥相關論文，不幸於 2008 年 3 月病逝，本次大會特別另設一專題來紀念他。

Properties of Injectable Calcium Silicate Hybrid Cements

Shinn-Jyh Ding, Chun-Cheng Chen, Wei-Chung Wang

Institute of Oral Biology and Biomaterials Science, Chung-Shan Medical University, Taichung 402,
Taiwan, R.O.C.

Introduction

Calcium silicate-based ceramics, such as CaSiO_3 , Ca_2SiO_4 , and bioactive glass, are good bioactive materials for bone defect repair in orthopedic and dental surgery. Self-setting calcium silicate cements (CSCs) can be handled by the surgeon in paste form and injected into bone cavities or defects. However, it is possible to difficultly deliver to the required site and hard to compact adequately due to relatively poor brittleness resistance. The polymeric materials may have the potential to improve the handling properties of CSCs due to excellent cohesion properties. Gelatin and chitosan are natural materials and have been widely employed as scaffolds and carrier. The aim of this study is to examine the effect of gelatin and chitosan on physical and chemical properties of CSCs.

Materials and Methods

The sol-gel method was used to prepare calcium silicate ceramics [1]. Briefly, tetraethyl orthosilicate and calcium nitrate were used as precursors for SiO_2 and CaO , respectively. Nitric acid was implemented as a catalyst and ethanol as a solvent. The nominal molar ratios of SiO_2/CaO ranged from 7/3 to 3/7. The sol solution was aged at 60°C for 1 day. After vaporization of the solvent in an oven at 120°C , the as-dried gel was heated in air to 800°C at a heating rate of $10^\circ\text{C}/\text{min}$ for 2 h, and then cooled to room temperature. 5 wt% gelatin powders were added to the sintered powders and the mixtures were ball-milled for 12 h. To prepare the cement, water or 5 wt% chitosan solution (chitosan oligosaccharide lactate) was used as liquid phases and the liquid-to-powder ratio was around 0.5, dependent on the Si/Ca ratio. A simulated body fluid (SBF) was used for *in vitro* bioactivity. X-ray diffractometer (XRD), Fourier transform infrared spectroscopy (FTIR), and scanning electron microscope (SEM) were used to characterize the specimens. The diametral tensile testing and injectability of cement samples was conducted. One-way analysis of variance (ANOVA) was used to evaluate the significant differences between the means in the DTS or setting time data. The results were considered statistically significant at $p < 0.05$.

Results and Discussion

The resulting XRD patterns show that the phase evolution depended on the Si/Ca molar ratio of the precursor materials. When containing the highest amount of SiO_2 , only amorphous phase appeared. In contrast, β -dicalcium silicate ($\beta\text{-Ca}_2\text{SiO}_4$) phases, which peak intensities increased with the increasing $\text{Ca}(\text{NO}_3)_2$ content of the precursor were found for the other specimens. In addition, the CaO peak intensities at $2\theta = 37.5^\circ$, increased with a trend similar to $\beta\text{-Ca}_2\text{SiO}_4$. The trends in the FTIR spectra of the as-sintered powders were similar to those indicated by XRD.

When the liquid phase was added to the solid phase, the product of the hydration process was a calcium silicate hydrate gel (C-S-H) because of a peak at $2\theta = 29.3^\circ$. The presence of chitosan in the cement specimen reduced the peak intensity of C-S-H, possibly due to its amorphous structure. From SEM observation, all ground powders are irregularly-shaped, having sizes smaller than $1\ \mu\text{m}$. When mixed with liquid phase, it seems to be the formation of entangled platelike crystals and exhibited several pores. It is well-known that if the powder and the liquid are mixed in an appropriate ratio, they form a paste that at room or body temperature hardens by entanglement of the crystals precipitated within the paste.

The setting time is one of important factors in clinical requirement. With the increase in the concentration of calcium component, the setting time of the cement became shorter, reaching 10 min, demonstrating the acceleration role of calcium in setting reaction. A long setting time could

cause problems clinically because of the cement's inability to maintain shape and support stresses within this time period. Interestingly, the addition of gelatin slightly increased the setting time, not for the chitosan. As for diametral tensile strength, the variations in the strength of various cements were found to also depend on the calcium amounts. One-way ANOVA analysis showed that there are statistically significant differences ($p < 0.05$). Gelatin or chitosan led to the decrease in the DTS of the cement specimens. It is worth noting that the highest DTS value is 2.8 MPa that belongs to the cement of $\text{CaO}/\text{SiO}_2 = 1$, which values reduced to 2.1 and 2.5 MPa when adding gelatin and chitosan into the cement, respectively. However, both gelatin and chitosan can greatly improve the injectability of the cement specimens, in particular, for gelatin.

DTS of immersed cement specimens had a greater value than the hardened cements, possibly due to the formation of more C–S–H gel in part. For example, the cement of $\text{CaO}/\text{SiO}_2 = 1$ increased two times after 1 day soaking in SBF. After soaking in SBF for as little as 1 day, all cements with and without gelatin and chitosan induced the precipitation of apatite spherulites, indicating their high bioactivity.

Conclusions

The calcium silicate-based hybrid cement could self-harden to form C–S–H gel. Gelatin and/or chitosan increased the setting time and reduced the strength, but they could improve the injectability. The cement specimens having equimolar amounts of CaO and SiO_2 had the highest DTS value of 2.8 MPa. Soaking in SBF led to the increase in the DTS of the cement specimens compared with the as-set specimens. All cements may promote the precipitation of a “bone-like” HA layer on the cement surfaces when exposed to a SBF, which may support their ability to integrate with living tissue.

Reference

1. Ding SJ, Shie MY, Wang CY. J Mater Chem, DOI: 10.1039/B819033J, 2009.

無研發成果推廣資料

國科會補助專題研究計畫成果報告自評表

請就研究內容與原計畫相符程度、達成預期目標情況、研究成果之學術或應用價值（簡要敘述成果所代表之意義、價值、影響或進一步發展之可能性）、是否適合在學術期刊發表或申請專利、主要發現或其他有關價值等，作一綜合評估。

1. 請就研究內容與原計畫相符程度、達成預期目標情況作一綜合評估

達成目標

未達成目標（請說明，以 100 字為限）

實驗失敗

因故實驗中斷

其他原因

說明：

2. 研究成果在學術期刊發表或申請專利等情形：

論文： 已發表 未發表之文稿 撰寫中 無

專利： 已獲得 申請中 無

技轉： 已技轉 洽談中 無

其他：（以 100 字為限）

3. 請依學術成就、技術創新、社會影響等方面，評估研究成果之學術或應用價值（簡要敘述成果所代表之意義、價值、影響或進一步發展之可能性）（以 500 字為限）

本計畫開發出的快速硬化型矽酸鈣骨水泥具高生物活性及骨形成性，添加可吸收高分子後更具注射性與抗沖蝕性，此種有機-無機混合骨水泥可作為複雜性骨修補使用，在臨床實用上，有其一定應用價值。藉此新材料開發可減少國內醫療器材與裝置的進口依賴，兼而提升國內醫療產品開發能力，甚至期許將產品推向國際舞台，目前已有國外廠商對此材料有興趣。本成果除已申請國內專利之外，也申請美國專利。

